

Allyl Amination of Phosphinoquinoline Allyl Complexes of Palladium. Influence of the Allyl Hapticity on the Reaction Rate and Regiochemistry

L. Canovese,^{*,†} F. Visentin,[†] C. Santo,[†] G. Chessa,[†] and V. Bertolasi[‡]

[†]Dipartimento di Chimica, Università Ca' Foscari, Venice, Italy, and [‡]Dipartimento di Chimica and Centro di Strutturistica Diffraattometrica Università di Ferrara, Ferrara, Italy

Received April 19, 2010

The ligands 8-diphenylphosphanylquinoline (DPPQ) and 8-diphenylphosphanyl-2-methylquinoline (DPPQ-Me) react in chlorinated solvents with the allyl dimers $[\text{Pd}(\mu\text{-Cl})(\eta^3\text{-C}_3\text{H}_5)_2]$ and $[\text{Pd}(\mu\text{-Cl})(\eta^3\text{-C}_3\text{H}_5\text{Me}_2)_2]$, yielding palladium allyl phosphanylquinoline complexes whose structure is strongly influenced by the ancillary ligand and the presence or the absence of chloride ion in solution. Thus, the allyl fragments in the DPPQ derivatives assume η^3 -hapticity in the absence of chloride and display monohapto coordination when the chloride is not removed from the reaction mixture. In the DPPQ-Me allyl derivatives the allyl fragment is always η^3 -coordinated, while the ancillary ligand may act as bis- or monochelating in the absence or in the presence of chloride, respectively. The reactivity of the allyl complexes was tested by means of the allyl-amination reaction carried out by either NMR or UV–vis techniques. It was noticed that the η^3 -derivatives generally display a higher reactivity than their η^1 -allyl analogues, under the same experimental conditions. It is apparent that chloride in chlorinated solvents is a quite good nucleophile, and therefore it may force the allyl moiety to assume the monohapto coordination or partially displace the hemilabile bis-chelate DPPQ-Me ligand. This experimental finding was also theoretically confirmed by means of an *ab initio* DFT computation. The crystal structures of the complexes $[\text{Pd}(\eta^3\text{-C}_3\text{H}_5)(\text{DPPQ})\text{ClO}_4]$ and $[\text{Pd}(\eta^1\text{-C}_3\text{H}_5)(\text{DPPQ})\text{Cl}]$ were resolved. The latter represents the seventh structure of a palladium complex with a σ -coordinated allyl fragment described in the literature.

Introduction

The nucleophilic attack by “soft” nucleophiles, which usually occurs at the terminal carbon of the η^3 -coordinated allyl fragment in palladium complexes, has been extensively studied and reviewed, since this reaction represents an important methodology in the vast field of palladium-catalyzed organic synthesis.¹ In some cases different reaction products due to nucleophilic attacks governed by different stereo-² and regioselectivity³ were proposed. Moreover, the allyl hapticity can be somehow influenced, and it is well known that the monohapticity of the allyl

fragment may induce alternative and interesting mechanisms.⁴ The allyl fragment may be forced to assume the monohapto configuration by potentially terdentate ligands or under the action of strong nucleophiles.⁵ In particular, in the cases of terdentate ligands such as terpyridine and 2,6-(diphenylphosphonylmethyl)pyridine the synthesis of stable complexes allowed X-ray structural determination.^{5i,j} It is however noteworthy that the synthesis of remarkably stable species and their consequent X-ray structural determinations were possible also for complexes bearing phospho- or phosphonite(oxazoline) (P–N) bidentate or potentially terdentate bis(oxazoline)phenylphosphonite (NOPON) ligands^{5d–h} (in the latter case the NOPON acts as a bidentate ligand with an uncoordinated wing). Notably, all the η^1 -allyl complexes bearing bidentate PN or potentially terdentate NOPON were always associated with a chloride moiety, which, while occupying the third coordinative position, stabilizes such unusual allyl hapticity. The recent papers by Jutand and Amatore dealing

*To whom correspondence should be addressed. E-mail: cano@unive.it.

(1) (a) Trost, B. M. *Angew. Chem., Int. Ed. Engl.* **1989**, *28*, 1173–1192. (b) Godlesky, S. A. In *Comprehensive Organic Synthesis*; Trost, B. M., Fleming, I., Semmelbach, M. F., Eds.; Pergamon: Oxford, U.K., 1991; Vol. 4, p 585. (c) Tsuji, J. In *Palladium and Catalysts Innovation in Organic Synthesis*; Wiley: Chichester, U.K. 1995; p 290. (d) *Handbook of Organopalladium Chemistry for Organic Synthesis*; Negishi, E., Ed.; Wiley: New York, 2002. (e) *Metal-catalyzed Cross-coupling Reactions*; de Meijere, A., Diederich, F., Eds.; Wiley-VCH: Weinheim, 2004.

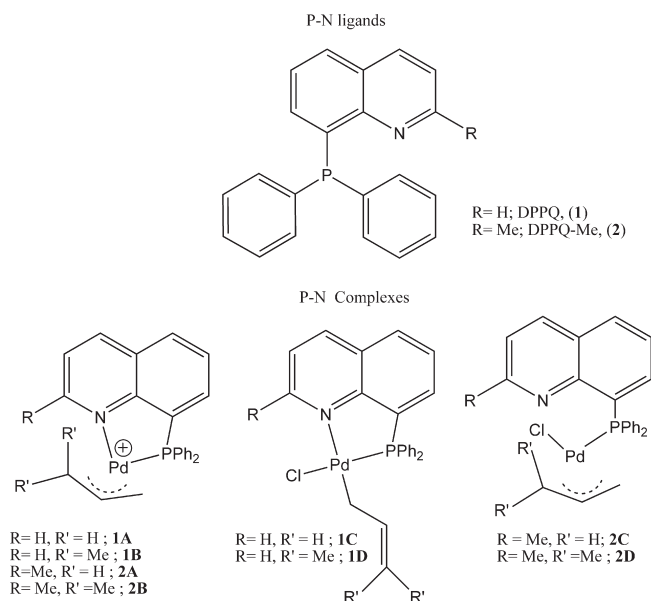
(2) (a) Togni, A.; Burkhardt, U.; Gramlich, V.; Pregosin, P. S.; Saltzmann, R. *J. Am. Chem. Soc.* **1996**, *118*, 1031–1037, and references therein. (b) Granberg, K. L.; Bäckvall, J. E. *J. Am. Chem. Soc.* **1992**, *114*, 6858–6863. (c) Trost, B. M.; Verhoeven, T. B. *J. Am. Chem. Soc.* **1980**, *102*, 4730–4743. (d) Trost, B. M.; Keinam, E. *J. Am. Chem. Soc.* **1978**, *100*, 7779–7781.

(3) Crociani, B.; Antonaroli, S.; Di Bianca, F.; Canovese, L.; Visentin, F.; Uguagliati, P. *J. Chem. Soc., Dalton Trans.* **1994**, 1145–1151, and references therein.

(4) (a) Cucciolito, M. E.; Vitagliano, A. *Organometallics* **2008**, *27*, 6360–6363. (b) Aydin, J.; Szabó, K. *Org. Lett.* **2008**, *10*, 2881–2884. (c) Piechaczyk, O.; Cantat, T.; Mézailles, N.; Le Floch, P. *J. Org. Chem.* **2007**, *72*, 4228–4237. (d) Kurosawa, H.; Urabe, A.; Miki, K.; Kasai, N. *Organometallics* **1986**, *5*, 2002–2008.

(5) (a) Canovese, L.; Visentin, F.; Santo, C.; Levi, C. *Organometallics* **2009**, *28*, 6762–6770. (b) Garcia-Iglesias, M.; Buñuel, E.; Cárdenas, D. *J. Organometallics* **2006**, *25*, 3611–3618, and references therein. (c) Jutand, A. *Appl. Organomet. Chem.* **2004**, *18*, 574–582, and references therein. (d) Zhang, J.; Braunstein, P.; Welter, R. *Inorg. Chem.* **2004**, *43*, 4172–4177. (e) Goldfuss, B.; Löschmann, T.; Rominger, F. *Chem.—Eur. J.* **2004**, *10*, 5422–5431. (f) Braunstein, P.; Zhang, J.; Welter, R. *Dalton Trans.* **2003**, 507–509. (g) Kollmar, M.; Helmchen, G. *Organometallics* **2002**, *21*, 4771–4775. (h) Braunstein, P.; Naud, F.; Dedieu, A.; Rohmer, M.-M.; DeCian, A.; Rettig, S. *J. Organometallics* **2001**, *20*, 2966–2981. (i) Barloy, L.; Ramdeehul, S.; Osborn, J. A.; Carloti, C.; Taulelle, F.; DeCian, A.; Fischer, J. *Eur. J. Inorg. Chem.* **2000**, 2523–2532. (j) Ramdeehul, S.; Barloy, L.; Osborn, J. A.; DeCian, A.; Fischer, J. *Organometallics* **1996**, *15*, 5442–5444.

Scheme 1



with the role of the “not-innocent” chloride when the palladium-catalyzed reactions are taken into consideration,^{5c,6} the original work of Akermark pointing out the possibility of the alternative nucleophilic attack at a η^1 -coordinate allyl group (S_N2' , S_N2),⁷ and finally our recent study on the thermodynamic aspects of the migratory insertion of the allyl group in palladium isocyanide complexes^{5a} drove us to plan an exhaustive investigation on the nature and the features of some η^1 -allyl complexes. We have thus undertaken the present study with the aim of contributing to the comprehension of the factors that might determine the allyl hapticity and of the overall reactivity and regioselectivity of such complexes when involved in reactions of allyl amination. We have chosen the allyl amination as reference reaction owing to its appropriate rate and the easy monitoring of the reaction progress.^{3,8} The complexes studied are summarized in Scheme 1.

Result and Discussion

General Remarks. When the dimers $[\text{Pd}(\mu\text{-Cl})(\eta^3\text{-C}_3\text{H}_3\text{-R}_2)]_2$ (R = H, Me) react in chlorinated solvents with two equivalents of the ligands DPPQ (**1**) and DPPQ-Me (**2**), we can anticipate that two different compounds were obtained according to the reactions reported in Scheme 2.

Irrespective of the allyl substituents R', both products are neutral with chloride coordinated to the palladium center. However, the allyl fragment in the DPPQ derivative is η^1 -coordinated, while in the DPPQ-Me complex it adopts

Scheme 2

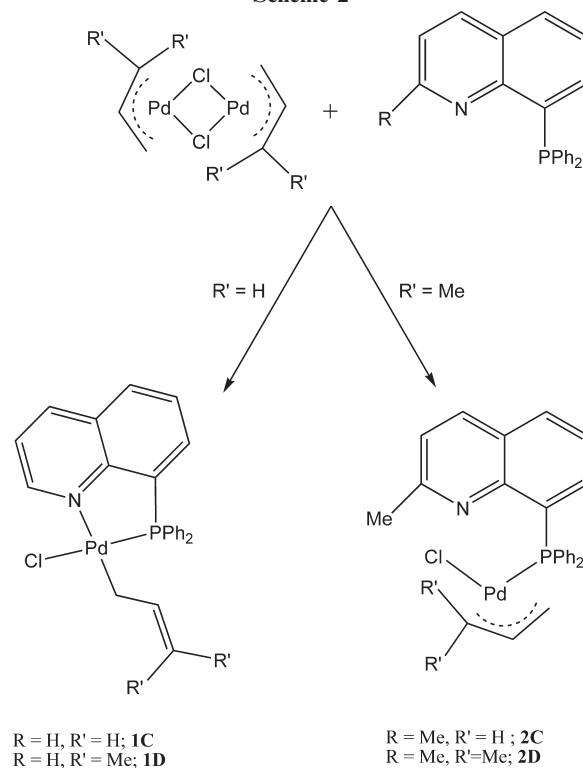
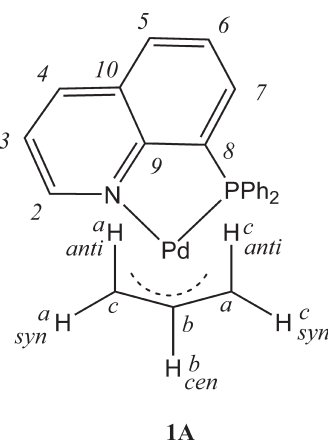


Chart 1



η^3 -hapticity with the consequent decoordination of the quinoline nitrogen.

The reactions in Scheme 2 can also be carried out in mixed solvent ($\text{CH}_2\text{Cl}_2/\text{MeOH}$) in the presence of the dechlorinating agent NaClO_4 . In these cases upon separation of NaCl and irrespectively of the nature of R and R', the reactions always yield the cationic species **1A**, **1B**, **2A**, and **2B** ($[\text{Pd}(\eta^3\text{-C}_3\text{H}_3\text{R}_2)(\text{DPPQ-R}')]^+$; R = H, Me; R' = H, Me).

Characterization and Properties of the Allyl Complexes.

For the sake of clarity, it is convenient to describe the characterization and the solution behavior of all the studied complexes when they bear the same ancillary ligand and allyl fragment in the absence and in the presence of the chloride ion.

(i) We have already stated that the reaction between the dimer $[\text{Pd}(\mu\text{-Cl})(\eta^3\text{-C}_3\text{H}_5)]_2$ and the ligand DPPQ (**1**) carried out in the presence of NaClO_4 yields the cationic complex **1A**, topologically represented together with its numbering scheme in Chart 1.

(6) (a) Cantat, T.; Agenet, N.; Jutand, A.; Pleixats, R.; Moreno-Mañas, M. *Eur. J. Org. Chem.* **2005**, 4277–4286. (b) Cantat, T.; Génin, E.; Giroud, C.; Meyer, G.; Jutand, A. *J. Organomet. Chem.* **2003**, 687, 365–376. (c) Amatore, C.; Jutand, A.; M'Barki, M. A.; Meyer, G.; Mottier, L. *Eur. J. Inorg. Chem.* **2001**, 873–880.

(7) Akermark, B.; Hegedus, L. S.; Zetterberg, K. *J. Am. Chem. Soc.* **1981**, 103, 3037–3040.

(8) (a) Crociani, B.; Antonaroli, S.; Canovese, L.; Visentin, F.; Uguagliati, P. *Inorg. Chim. Acta* **2001**, 315, 172–182. (b) Crociani, B.; Antonaroli, S.; Bandoli, G.; Canovese, L.; Visentin, F.; Uguagliati, P. *Organometallics* **1999**, 18, 1137–1147, and references therein. (c) Canovese, L.; Visentin, F.; Uguagliati, P.; Chessa, G.; Lucchini, V.; Bandoli, G. *Inorg. Chim. Acta* **1998**, 275–276, 385–394. (d) Canovese, L.; Visentin, F.; Uguagliati, P.; Chessa, G.; Pesce, A. *J. Organomet. Chem.* **1998**, 566, 61–71. (e) Canovese, L.; Visentin, F.; Uguagliati, P.; Chessa, G.; Crociani, B.; Di Bianca, F. *Inorg. Chim. Acta* **1995**, 235, 45–50. (f) Canovese, L.; Visentin, F.; Uguagliati, P.; Di Bianca, F.; Antonaroli, S.; Crociani, B. *J. Chem. Soc., Dalton Trans.* **1994**, 3113–3118.

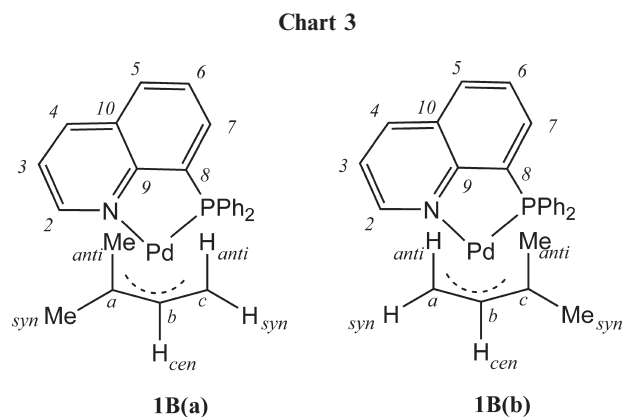
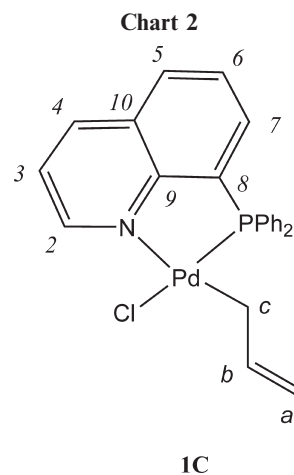
The low-temperature (213 K) ^1H NMR spectrum of complex **1A** in CD_2Cl_2 displays five groups of signals ascribable to allyl protons at 2.97, 4.08, 4.29, 5.04, and 6.03 ppm. The doublets at 2.97 and 4.04 ppm are due to the H^c_{anti} and H^c_{syn} coupling (protons in *trans* position with respect to the quinoline nitrogen atom), the doublets of doublets at 4.29 and 5.05 ppm are ascribable to the H^a_{anti} and H^a_{syn} coupling with the phosphorus atom in *trans* position, while the multiplet at 6.03 ppm is due to the central allyl proton H^b_{cen} coupling with four inequivalent protons.

On increasing the temperature (298 K), the massive broadening of the signals of the protons H^c is observed. This phenomenon is due to the well-known selective *syn-anti* isomerism that is traceable back to a $\eta^3-\eta^1-\eta^3$ fluxionality.^{5i,9} Notably, such a phenomenon is triggered by the remarkable *trans*-labilizing influence of phosphorus.

The RT $^{13}\text{C}\{^1\text{H}\}$ NMR confirms the labilization of the allyl carbon (C^c) in *trans* position to phosphorus, which resonates as a doublet at 83.2 ppm, while the C^c resonates at higher field (51.9 ppm). The position of the signal ascribable to the central carbon atom (C^b) is about 120 ppm, which represents a predictable frequency for this type of allyl derivative.

(ii) The CD_2Cl_2 ^1H NMR spectrum at 213 K of the derivative **1C** obtained by adding the ligand DPPQ (**1**) to a CH_2Cl_2 solution of $[\text{Pd}(\mu\text{-Cl})(\eta^3\text{-C}_3\text{H}_5)]_2$ without subsequent dechlorination of the solution (no NaClO_4 addition) displays a quite different behavior. In this case only four groups of signals ascribable to the allylic protons can be noticed, at 2.61, 4.04, 4.32, and 6.09 ppm. The high-field signal (doublet of doublets; $J_{\text{HH}} = 8.2$, $J_{\text{HP}} = 4.1$ Hz) is ascribable to two equivalent protons of the carbon directly coordinated to the palladium belonging to a η^1 -coordinated allyl fragment in *cis* position to a phosphorus atom. The corresponding carbon (C^c) resonates at about 20 ppm in the $^{13}\text{C}\{^1\text{H}\}$ NMR spectrum, thereby indicating the alkylic nature of the carbon directly coordinated to the metal.^{5e,f} The couple of doublets at 4.04 and 4.32 ppm are traceable back to the protons *trans* ($J_{\text{HH}} = 17.1$ Hz) and *cis* ($J_{\text{HH}} = 9.9$ Hz) to the central proton H^b , which resonates as a multiplet at 6.09 ppm. Moreover, the position of the signals due to the central and terminal carbon in the η^1 complex differs substantially from those of the η^3 -species (see Experimental Section). The fourth coordinative position is occupied by a chloride, which induces a remarkable deshielding of the quinoline H^2 proton that resonate at a quite low field (9.89 ppm). This phenomenon, which has been already observed,¹⁰ is probably due to an anisotropic effect. Notably, a similar outcome is observed also in complexes bearing halogen atoms coordinated to pyridylthioether methyl palladium species in which the deshielding extent is influenced by the nature of the halide ($\text{I}^- > \text{Br}^- > \text{Cl}^-$).^{10b} Coordination of the chloride is also supported by the IR spectrum, which, at variance with complex **1A**, displays a Pd–Cl stretching at 272 cm^{-1} , but mainly by the structural characterization of the complex **1C** (*vide post*).

Interestingly, complex **1C** displays a $\eta^1-\eta^3-\eta^1$ fluxional rearrangement as a consequence of the increasing temperature. Such a phenomenon is not so frequent and to the best of our knowledge was observed in one more case.⁵ⁱ As a matter of fact, the ^1H NMR spectrum at 298 K shows the partial coalescence of the terminal allyl protons, which completely



collapse at 353 K ($\text{C}_2\text{D}_2\text{Cl}_4$). At this temperature the signal of the four terminal allyl protons becomes a broad singlet at 3.75 ppm, while the central allyl proton resonates as a sharp quintet (see Supporting Information: Figure 2 SI).

(iii) The reaction of the ligand DPPQ (**1**) with the dimer $[\text{Pd}(\mu\text{-Cl})(\eta^3\text{-C}_3\text{H}_3\text{Me}_2)]_2$ in chlorinated solvents in the presence of NaClO_4 yields the complex **1B**, which can be isolated as a couple of diastereoisomers (**1B(a)**/**1B(b)** = 1.4:1) (Chart 3)

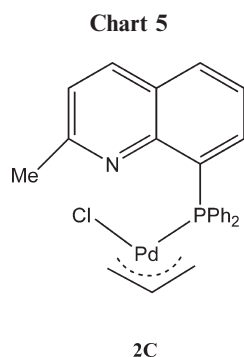
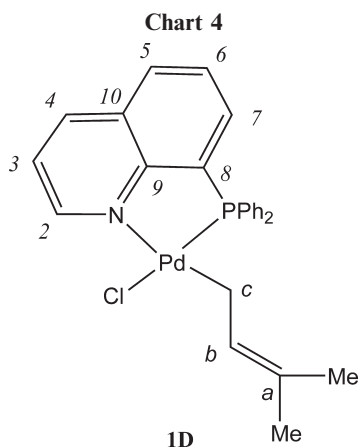
The isomeric ratio can be easily inferred from the ^1H NMR spectra in CD_2Cl_2 at 253 K of the isomeric mixture in which only the *syn* and *anti* protons *trans* to phosphorus give rise to two doublets of doublets at 4.74 and 4.22 ppm, respectively (see Experimental Section).

(iv) The reaction between the dimer $[\text{Pd}(\mu\text{-Cl})(\eta^3\text{-C}_3\text{H}_3\text{Me}_2)]_2$ and the ligand DPPQ (**1**) carried out without dechlorinating agents yields the complex **1D**. As expected, in analogy with the previous results, the complex **1D** displays the allyl fragment σ coordinated to palladium via the less substituted carbon (η^1 hapticity) (Chart 4)

As in the previously described complex **1C**, the ^1H and ^{13}C NMR spectra of complex **1D** suggest the allyl monohapticity. In particular the doublet of doublets at 2.89 ppm is traceable back to the protons bonded to the C^c carbon of the allyl fragment coupling with the allyl central proton and with the phosphorus in *cis* position ($J_{\text{HP}} \approx 3$ Hz). The high-field resonance of the allyl carbon C^c ($\delta = 15.6$ ppm), the proximity of the C^a -coordinated methyl protons signals ($\Delta\delta = 0.21$ ppm), which is not unprecedented^{5a} and not consistent with that of geminal methyl groups of a η^3 -coordinated 1,1-dimethylallyl, and the low-field resonance of the H^2 quinoline proton (10.03 ppm) strongly suggest the structure depicted in Chart 4 for the complex **1D**.

(9) Canovese, L.; Visentin, F.; Uguagliati, P.; Lucchini, V.; Bandoli, G. *Inorg. Chim. Acta* **1998**, *277*, 247–252.

(10) (a) Canovese, L.; Visentin, F.; Chessa, G.; Uguagliati, P.; Bandoli, G. *Organometallics* **2000**, *19*, 1461–1463. (b) Canovese, L.; Chessa, G.; Santo, C.; Visentin, F.; Uguagliati, P. *Inorg. Chim. Acta* **2003**, *346*, 158–168.



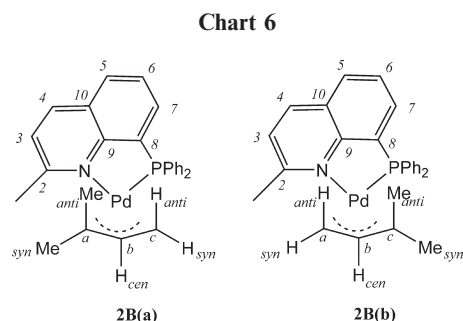
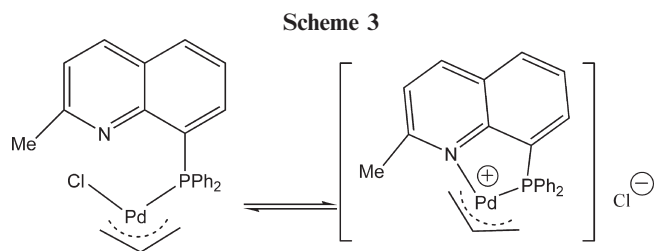
(v) The reaction between the ligand DPPQ-Me (**2**) and the allyl dimer $[\text{Pd}(\mu\text{-Cl})(\eta^3\text{-C}_3\text{H}_5)]_2$ in the absence of chloride yields the 3-hapto derivative $[\text{Pd}(\eta^3\text{-C}_3\text{H}_5)(\text{DPPQ-Me})]$ (**2A**), which behaves similarly to its DPPQ analogue. As a matter of fact, the NMR spectra of the two derivatives look very similar, and the selective *syn-anti* isomerization ($\eta^3\text{-}\eta^1\text{-}\eta^3$) is operative in this case also.

(vi) The same reaction carried out in the presence of chloride gives the species $[\text{Pd}(\eta^3\text{-C}_3\text{H}_5)(\kappa^1\text{-DPPQ-Me})\text{Cl}]$ (**2C**), which is topologically represented in Chart 5

The structure in Chart 5 clearly emerges from analysis of the 298 K ^1H and ^{13}C NMR spectra of complex **2C** and might be somehow referred to that of the complex $[\text{Pd}(\eta^3\text{-C}_3\text{H}_5\text{-Me}_2)(\text{dmphen})]$, which displays a marked asymmetry between the two Pd-N bonds.¹¹

The terminal allyl protons resonate at 3.65 ppm as a doublet of doublets with $J_{\text{HH}} = 10$ and $J_{\text{HP}} = 3.9$ Hz, which represent a reasonable average of the coupling constants among the *anti* and the *syn* protons with the central allyl protons and the phosphorus atom, respectively, while the central allyl proton resonates as a well-resolved quintet at 5.67 ppm ($J_{\text{HH}} = 10$ Hz). Accordingly, the ^{13}C NMR spectrum at the same temperature (298 K) displays a unique signal for the terminal carbons at 68 ppm (reasonable average between the signals of one carbon *trans* to phosphorus and another *trans* to chloride), while the central carbon assumes the typical position of a η^3 -allyl system at about 118 ppm ($J_{\text{CP}} = 5.8$ Hz).¹²

The observed behavior is traceable back to the extensive fluxional phenomena (typically *syn-anti* and *syn-syn anti-anti*



rearrangements) usually induced by the presence of adventitious nucleophiles.^{8b} Apparently, in this case the role of the nucleophile is fulfilled by the quinoline nitrogen of the uncoordinated wing.

Further evidence on the structure of complex **2C** is given by the resonance of the methyl protons in position 2 of the quinoline ring. These protons resonate at 2.71 ppm, which is very near the resonance of the same protons of the uncoordinated DPPQ-Me (2.60 ppm) and at a quite different field if compared with the resonance of the bis-coordinate ligand (i.e., the methyl protons in the case of the dechlorinated complex $[\text{Pd}(\eta^3\text{-C}_3\text{H}_5)(\text{DPPQ-Me})]$ (**2A**) resonate at 3.11 ppm; see Experimental Section). From the NMR spectra at low temperature (178 K) it is possible to deduce that a further process takes place. On decreasing the temperature, the ^{31}P signal significantly shifts from 22.7 to 32.0 ppm. Moreover, the ^1H NMR at the same temperature can be interpreted on the basis of the formation of the complex $[\text{Pd}(\eta^3\text{-C}_3\text{H}_5)(\text{DPPQ-Me})]^+\text{Cl}^-$, in which the DPPQ-Me moiety acts again as a bidentate ligand (see Supporting Information: Figure 7 SI).

Apparently, the equilibrium reported in Scheme 3 between the neutral and the cationic allyl complexes takes place.

(vii) The reaction between the dimer $[\text{Pd}(\mu\text{-Cl})(\eta^3\text{-C}_3\text{H}_5\text{-Me}_2)]_2$ and the ligand DPPQ-Me (**2**) in the presence of NaClO_4 at 298 K yields the diastereoisomers depicted in Chart 6.

At variance with the case related to complex **1B**, the isomer **2B(b)** represents the most abundant species ($\mathbf{2B(b)/2B(a)} = 2.3:1$) probably due to the mutual steric interference exerted by the methyl groups of the allyl fragment and of the quinoline ring. Notably, the equilibrium between isomers is influenced by temperature, and at 198 K the ratio becomes $\mathbf{2B(b)/2B(a)} = 6.3:1$.

(viii) The same reaction carried out in the presence of chloride yields complex **2D**, which is present in solution only as the isomer bearing the allylic methyl groups in *trans* position to the phosphorus atom (see Chart 7).

As a matter of fact, the ^1H and ^{13}C NMR spectra in CD_2Cl_2 at 298 K strongly suggest this conclusion. The central allyl proton, which resonates as a triplet at 5.19 ppm, is coupled with the allyl terminal protons resonating as a doublet at 2.75 ppm. The coupling constant $J_{\text{HH}} = 9.8$ Hz represents the average between one *syn* and one *anti* proton *trans* to chloride. This observation suggests that the *syn-anti* selective isomerism rules out the formation of an allyl group η^1 -coordinated to the palladium via the most substituted terminal carbon. The allyl methyl

(11) Hansson, S.; Norrby, P.-O.; Sjögren, M. P. T.; Åkermark, B.; Cucciolito, M. E.; Giordano, F.; Vitagliano, A. *Organometallics* **1993**, *12*, 4940–4948.

(12) Åkermark, B.; Krakenberg, B.; Hansson, S.; Vitagliano, A. *Organometallics* **1987**, *6*, 620–628.

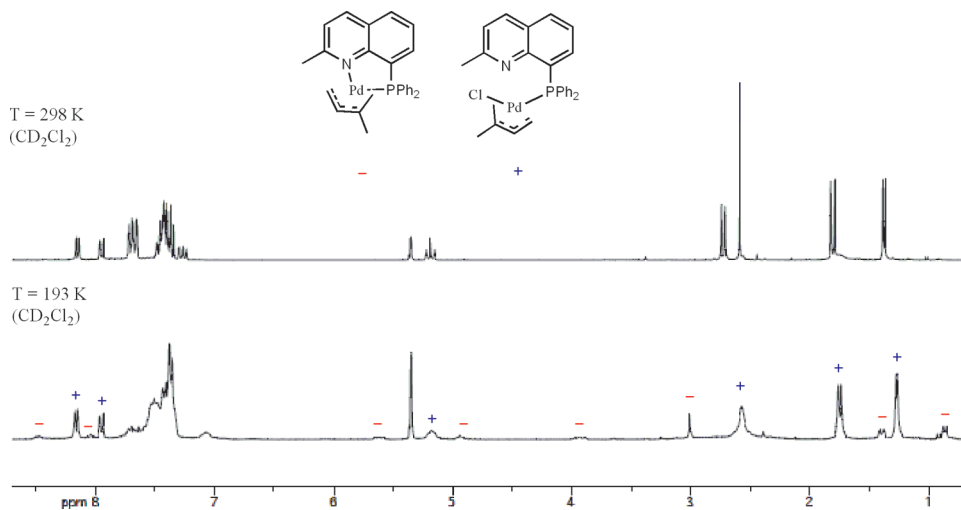
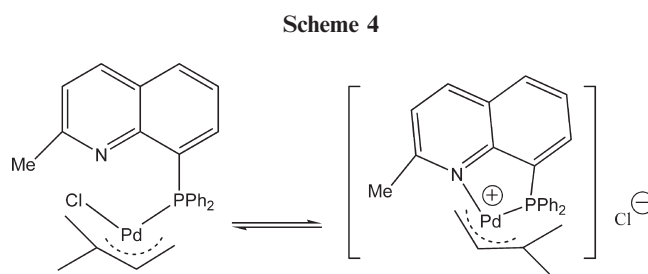
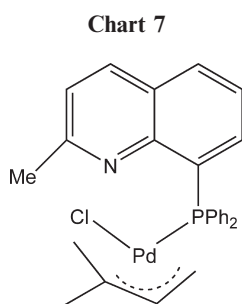


Figure 1. ^1H NMR spectra in CD_2Cl_2 of complex **2D** at different temperatures.



groups resonate as two doublets at 1.37 and 1.80 ppm since they are coupled with the phosphorus in *trans* position. The ^{13}C NMR spectrum is in accord with these conclusions. In particular, the less substituted terminal carbon resonates at 48.9 ppm, which represents a reasonable frequency for a carbon *trans* to chlorine, while the signal of the most substituted quaternary carbon is found as a doublet ($J_{\text{CP}} = 25$ Hz) at 114 ppm.

As can be deduced from Figure 1, a decreasing temperature favors the establishment of the equilibrium in Scheme 5. However, probably due to the inadequate instrumental sensitivity of the two possible isomers of the cationic complex $[\text{Pd}(\eta^3\text{-C}_3\text{H}_5\text{Me}_2)(\text{DPPQ-Me})^+\text{Cl}^-]$, only the derivative bearing the substituted allyl terminus *cis* to phosphorus was identified in solution at 193 K (see Scheme 4).

Computational Investigation. It has been observed that the ligands DPPQ and DPPQ-Me when reacting with the dimer $[\text{Pd}(\mu\text{-Cl})(\eta^3\text{-C}_3\text{H}_5)]_2$ in the presence of chloride surprisingly promote the formation of the complex $[\text{Pd}(\eta^1\text{-C}_3\text{H}_5)(\text{DPPQ})\text{Cl}]$ (**1A**) or $[\text{Pd}(\eta^3\text{-C}_3\text{H}_5)(\kappa^1\text{-DPPQ-Me})\text{Cl}]$ (**2C**). We have therefore resorted to a theoretical computational approach

based on an *ab initio* DFT method in order to better understand this peculiar difference in the ligand behavior.^{13,14} The computational response is depicted in Figure 2.

It is apparent that the theoretical evidence is in accord with the experimental results. Thus, the formation of the complex $[\text{Pd}(\eta^1\text{-C}_3\text{H}_5)(\text{DPPQ})\text{Cl}]$ (**1C**) is energetically favored if compared with that of the hypothetical complex $[\text{Pd}(\eta^3\text{-C}_3\text{H}_5)(\text{DPPQ})\text{Cl}]$, while the corresponding complexes bearing the ligand DPPQ-Me display an inversion in the energy levels. As a matter of fact, the distortion induced by the methyl substituent in the quinoline ring favors breaking of the N–Pd bond instead of reduction of the allyl hapticity ($\eta^3 \rightarrow \eta^1$). This destabilizing effect is well known and was previously observed in other palladium derivatives.^{10,15}

Crystal Structure Determinations. ORTEP¹⁶ views of the complexes **1C** and **1A** are shown in Figures 5 and 6. The Pd(II) complex **1C** exhibits square-planar coordination with the η^1 -allyl ligand *trans* to the nitrogen N1 of quinoline moiety. The Pd1–N1 bond length of 2.161(2) Å is in agreement with Pd–N (sp^2) distances in the range 2.13–2.18 Å of complexes having similar coordination geometries.^{5d–h} These bonds display a lengthening with respect to distances [2.06(2) Å, on average] in $[\text{Pd}(\text{P–N})\text{Cl}_2]$ complexes where the nitrogen is *trans* to a Cl,^{5c,17}

(13) Frisch, M. J.; Trucks, G. W.; Schlegel, H. B.; Scuseria, G. E.; Robb, M. A.; Cheeseman, J. R.; Scalmani, G.; Barone, V.; Mennucci, B.; Petersson, G. A.; Nakatsuji, H.; Caricato, M.; Li, X.; Hratchian, H. P.; Izmaylov, A. F.; Bloino, J.; Zheng, G.; Sonnenberg, J. L.; Hada, M.; Ehara, M.; Toyota, K.; Fukuda, R.; Hasegawa, J.; Ishida, M.; Nakajima, T.; Honda, Y.; Kitao, O.; Nakai, H.; Vreven, T.; Montgomery, J. A., Jr.; Peralta, J. E.; Ogliaro, F.; Bearpark, M.; Heyd, J. J.; Brothers, E.; Kudin, K. N.; Staroverov, V. N.; Kobayashi, R.; Normand, J.; Raghavachari, K.; Rendell, A.; Burant, J. C.; Iyengar, S. S.; Tomasi, J.; Cossi, M.; Rega, N.; Millam, J. M.; Klene, M.; Knox, J. E.; Cross, J. B.; Bakken, V.; Adamo, C.; Jaramillo, J.; Gomperts, R.; Stratmann, R. E.; Yazyev, O.; Austin, A. J.; Cammi, R.; Pomelli, C.; Ochterski, J. W.; Martin, R. L.; Morokuma, K.; Zakrzewski, V. G.; Voth, G. A.; Salvador, P.; Dannenberg, J. J.; Dapprich, S.; Daniels, A. D.; Farkas, O.; Foresman, J. B.; Ortiz, J. V.; Cioslowski, J.; Fox, D. J. *Gaussian 09*, Revision A.1; Gaussian, Inc.: Wallingford, CT, 2009.

(14) (a) Zhao, Y.; Truhlar, D. G. *Theor. Chem. Acc.* **2008**, *120*, 215–241. (b) Weigend, F.; Ahlrichs, R. *Phys. Chem. Chem. Phys.* **2005**, *7*, 3297–3305.

(15) Canovese, L.; Visentin, F.; Chessa, G.; Santo, C.; Dolmella, A. *Dalton Trans.* **2009**, 9475–9485.

(16) Burnett, M. N.; Johnson, C. K. *ORTEP III*, Report ORNL-6895; Oak Ridge National Laboratory: Oak Ridge, TN, 1996.

(17) (a) Shaffer, A. R.; Schmidt, J. A. R. *Organometallics* **2008**, *27*, 1259–1266. (b) Agostinho, M.; Banu, A.; Braunstein, P.; Welter, R.; Morise, X. *Acta Crystallogr. Sect. C* **2006**, *62*, m81–m86. (c) Ankersmit, H. A.; Løken, B. H.; Kooijman, H.; Spek, A. L.; Vrieze, K.; van Koten, G. *Inorg. Chim. Acta* **1996**, *252*, 141–155. (d) Apfelbacher, A.; Braunstein, P.; Brissieux, L.; Welter, R. *Dalton Trans.* **2003**, 1669–1674.

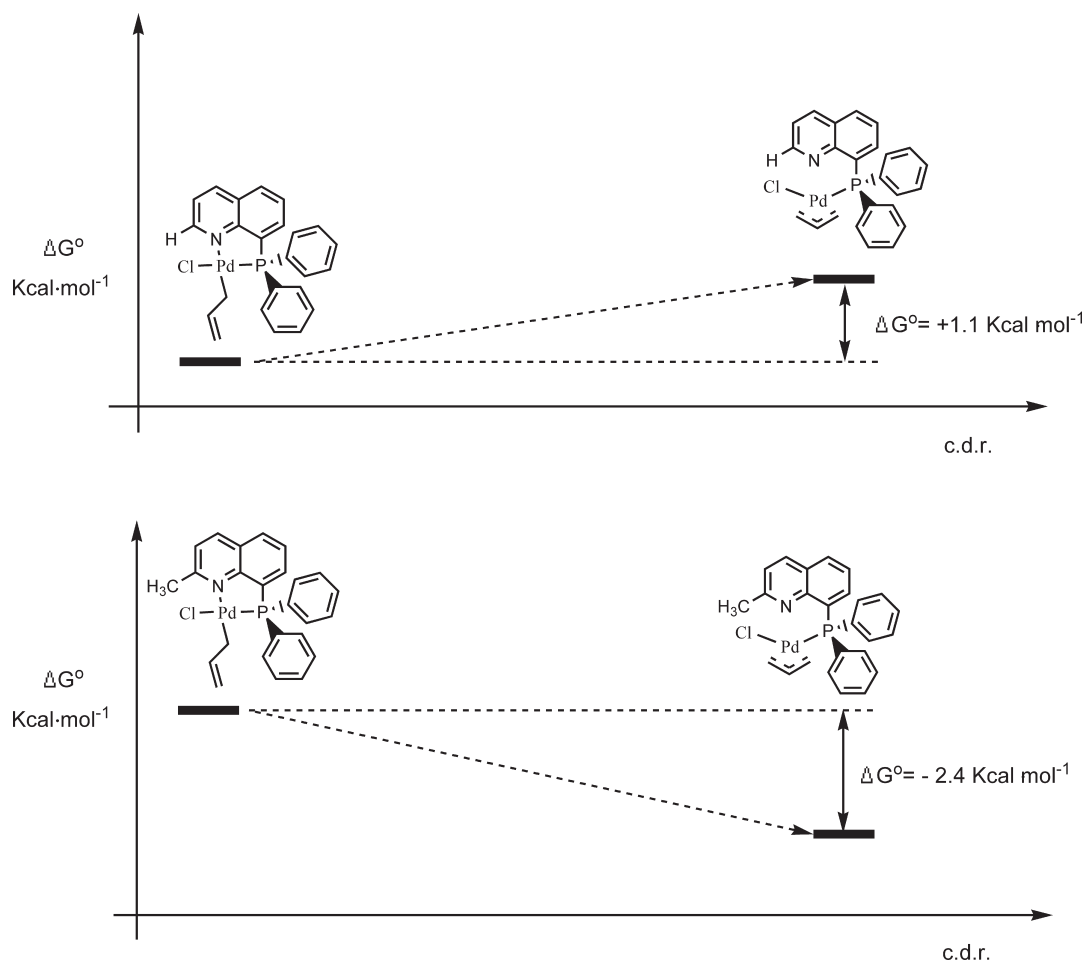
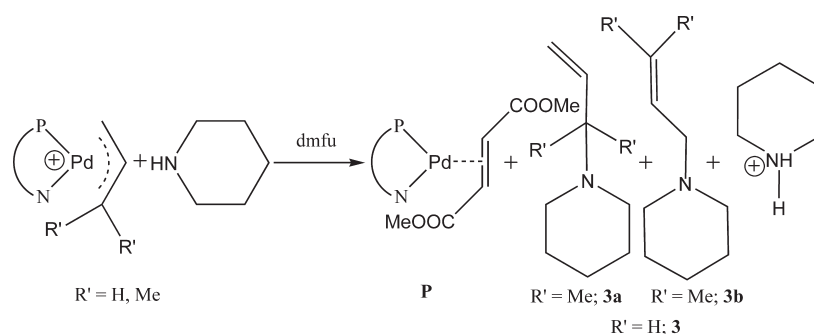


Figure 2. Calculated ΔG^0 of formation for the complexes $[\text{Pd}(\eta^3\text{-C}_3\text{H}_5)(\kappa^1\text{-DPPQ})\text{Cl}]$ and $[\text{Pd}(\eta^3\text{-C}_3\text{H}_5)(\kappa^1\text{-DPPQ-Me})\text{Cl}]$ (**2C**).

Scheme 5



showing that the η^1 -allyl group exerts on N a *trans* influence greater than Cl. The conformation of the coordinated η^1 -allyl group can be described by the torsion angles $\text{Pd}-\text{Cl}-\text{C}_2-\text{C}_3 = 110.6(4)^\circ$ and $\text{P}-\text{Pd}-\text{Cl}-\text{C}_2 = -109.1(2)^\circ$. The plane of the allyl group makes a dihedral angle of $69.6(3)^\circ$ with the mean coordination plane. The C_1-C_2 and C_2-C_3 bond distances of 1.454(4) and 1.319(5) Å clearly show a differentiation between single and double bonds and are within the ranges of distances of 1.45–1.47 and 1.30–1.37 Å, respectively, observed in allyl groups of $[\text{Pd}(\eta^1\text{-C}_3\text{H}_5)(\text{P}-\text{N})\text{Cl}]$ complexes.^{5d-h}

In cationic complex **1A** the palladium atom bonded to one nitrogen, one phosphorus, and two terminal η^3 -allylic carbon atoms shows a distorted-square-planar coordination. The greater *trans* influence exerted by the phosphine moiety as compared to the N(quinoline) group is evidenced by the Pd-terminal

η^3 -allyl carbon distances, which are longer *trans* to the P (2.214(4) Å) than *trans* to the N atom (2.107(4) Å). The same effect can be observed in other $[\text{Pd}(\eta^3\text{-C}_3\text{H}_5)(\text{P}-\text{N})]^+$ complexes,^{5c,f,17a,18} where Pd–C(*trans* to P) and Pd–C(*trans* to N) bond lengths display average values of 2.22(2) and 2.11(1) Å, respectively. The η^3 -coordinated allyl moiety, forming a dihedral angle of $56.6(7)^\circ$, is obliquely placed with respect to the metal square plane. The central C2 atom of the η^3 -allyl group is located above the mean coordination plane by 0.326(6) Å (Figure 5).

(18) (a) Mandal, S. K.; Gowda, G. A. N.; Krishnamurthy, S. S.; Nethaji, M. *Dalton Trans.* **2003**, 1016–1027. (b) Franco, D.; Gomez, M.; Jimenez, F.; Muller, G.; Rocamora, M.; Maestro, M. A.; Mahia, J. *Organometallics* **2004**, *23*, 3197–3209. (c) Pascu, S. I.; Coleman, K. S.; Cowley, A. R.; Green, M. L. H.; Rees, N. H. *J. Organomet. Chem.* **2005**, *690*, 1645–1658. (d) Faller, J. W.; Sarantopoulos, N. *Organometallics* **2004**, *23*, 2008–2014.

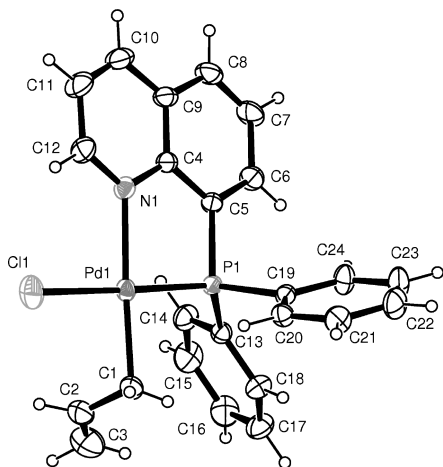


Figure 3. ORTEP view of complex **1C** showing the thermal ellipsoids at the 30% probability level.

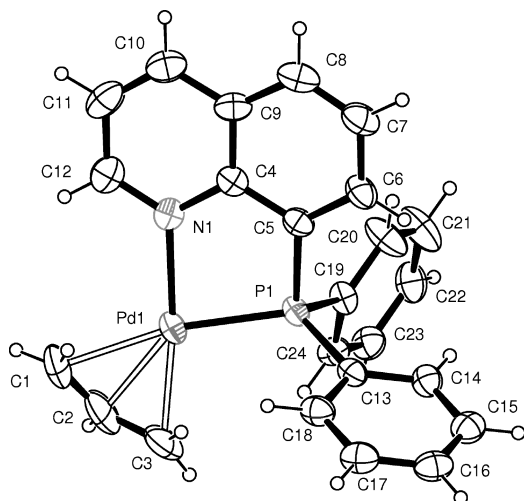


Figure 4. ORTEP view of the cationic complex **1A** showing the thermal ellipsoids at the 30% probability level.

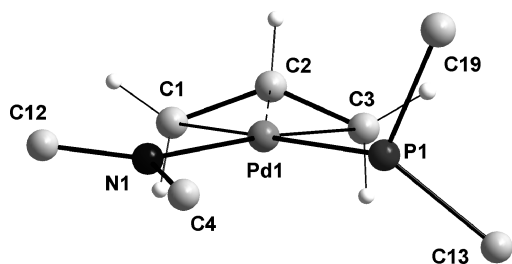


Figure 5. Orientation of the η^3 -allyl group with respect to the Pd coordination plane in **1A**.

Allyl Amination. Preliminary NMR Studies. Since complexes with different ligand organization might display different reactivity, we have decided to compare some of the complexes described by means of the allyl-amination reaction using piperidine as reference nucleophile in the presence of dimethylfumarate (dmfu), which stabilizes the palladium(0) residue (Scheme 5).

We have first monitored the reaction progress by ^1H and ^{31}P NMR techniques by adding an adequate quantity of piperidine and dmfu to a CD_2Cl_2 solution of the complexes under study at RT. In the case of complex **1A** the reaction

was over in about 4 min, while that of complex **1C** took more than 45 min to be complete. Evidently, the attack at the η^1 -allyl is disfavored with respect to that at the η^3 -coordinated allyl moiety. In both cases the reaction products were the palladium(0) derivative $[\text{Pd}(\eta^2\text{-dmfu})(\text{DPPQ})]$ (**P**), the 1-allylpiperidine (**3**), and the protonated piperidine. However, owing to the symmetry of the allyl fragment, no information on the site of attack and on the related rates could be gathered, although it may be suggested that attack of the piperidine takes place principally at the most electropositive terminal allyl carbon, which is *trans* to phosphorus¹² and at the allyl face opposite the palladium center.³ We have therefore resorted to the complexes **1B** and **1D** in an attempt to obtain deeper insight into the mechanism. The most evident piece of information we have obtained in these cases is given by the remarkable increase of reaction time. Under the same experimental conditions of concentration and temperature, the reaction of **1B** and **1D** with piperidine takes about 20 and 420 min, respectively. The ratio of rates is roughly maintained (4:45 to 20:420 min), but steric hindrance clearly plays an important role in determining the reaction rates in the case of associative mechanisms. Moreover, upon piperidine and dmfu addition, complex **1B** yields the usual derivative **P** and a 1:4 mixture of the compounds 1-(1,1-dimethylallyl)piperidine (**3a**) and 1-(3-methylbut-2-enyl)piperidine (**3b**) (**3a/3b** = 1:4). When the amination of the chlorinated η^1 -allyl complex **1D** is taken into consideration, an inversion in the regioselectivity is observed since the ratio between the allyl-amines becomes **3a/3b** = 2:1. It is well known that the presence of nucleophiles in solution causes an extensive fluxionality in palladium η^3 -allyl complexes.^{8b} Therefore the addition of piperidine to a solution of the complex **1B** might induce a fast isomerization process between the two possible isomers **1B(a)** and **1B(b)**, thereby enforcing the Curtin–Hammett regime.¹⁹ The kinetic solution of the system under study is however not possible, although the reasonable hypothesis that the most reactive species could be the **1B(b)** isomer might be advanced since this isomer has the less hindered allyl carbon *trans* to phosphorus. On the contrary, complex **1D** undergoes no isomeric rearrangements even under the action of piperidine. Consequently, it is evident that attack to both terminal carbons of the η^1 -allyl fragment is possible ($\text{S}_{\text{N}}2'$ and $\text{S}_{\text{N}}2$). Moreover, on the basis of the observed ratio of the concentrations of the allyl-amines **3a** and **3b** it may be deduced that the $\text{S}_{\text{N}}2'$ path represents the less energy demanding route to the products (Chart 8).

We have also monitored by the NMR technique the reaction of the complexes **2A** and **2C** with piperidine. The two complexes display a similar reactivity trend (*vide infra*) since the unsubstituted allyl fragment remains η^3 -coordinated in both derivatives.

Solvent Effect. The nucleophilic capability of halide ions toward palladium(II) in chlorinated solvents is well known and established,²⁰ and therefore the behavior of palladium allyl complexes in the presence of chloride is remarkably influenced by the nature of the solvent. Thus, solutions of the complexes **1A** and **1C** in CD_3OD display the same NMR spectra and exactly the same reaction rate when reacted with piperidine. Solvolysis depresses the nucleophilic capability of chloride and favors the re-establishment of the η^3 -hapticity

(19) Seeman, J. I. *Chem. Rev.* **1983**, *83*, 83–134.

(20) Canovese, L.; Chessa, G.; Santo, C.; Visentin, F.; Uguagliati, P. *Inorg. Chim. Acta* **2003**, *346*, 158–168.

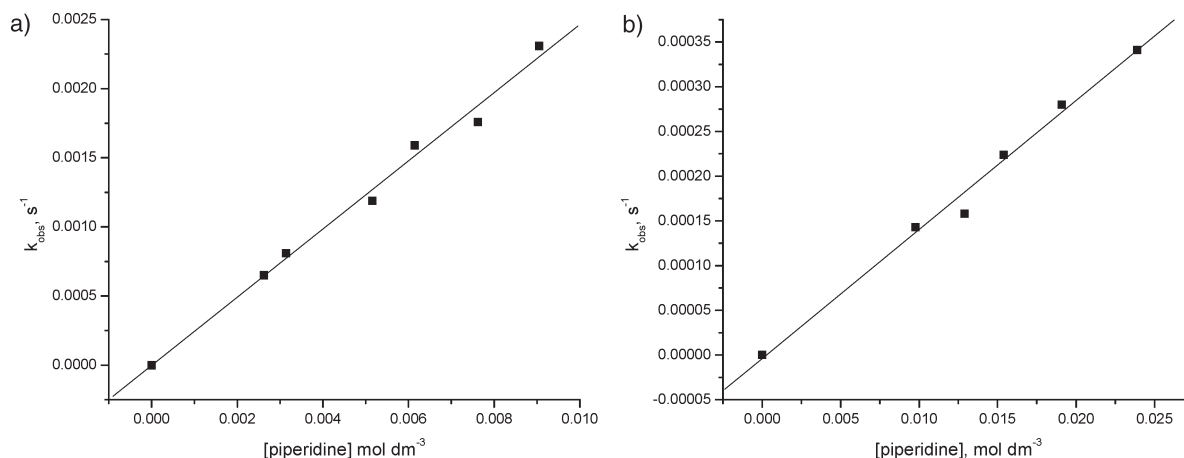
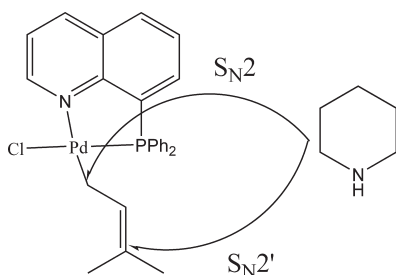


Figure 6. (a) Linear regression analysis for the reaction between complex **1A** and piperidine. (b) Linear regression analysis for the reaction between complex **1C** and piperidine.

Chart 8



of the allyl group. Thus, the two complexes are better described as the same species bearing different counterions ($[\text{Pd}(\eta^3\text{-C}_3\text{H}_5)(\text{DPPQ})]^+\text{X}^-$; $\text{X}^- = \text{Cl}^-, \text{ClO}_4^-$).

As expected, the reactivity of piperidine as a consequence of solvolysis is also lowered in methanol since its nucleophilic ability and the consequent reaction rate are depressed.

Spectrophotometric Studies. The spectrophotometric approach to the kinetic problems is often convenient since it combines a reduced experimental difficulty and a prompt response with a clear-cut determination. Moreover, the NMR outputs are not always superimposable to the UV–vis interpretations particularly when equilibrium reactions are involved. As a matter of fact, the different concentrations of the sample imposed by the two different techniques might severely affect the equilibrium position, and consequently the reproducibility of independent observations is not warranted.

In the case of spectrophotometric determinations, the accompanying high dilution of the starting chlorinated complexes (**1C**, **2C**) renders chloride dissociation and consequently the concentration of the cationic **1A** and **2A** significant.²¹ Thus, the complete mechanistic scheme related to piperidine attack to the allyl derivative in the case of an established equilibrium mixture between dechlorinated and chlorinated allyl complexes is more appropriately described by Scheme 6.⁸

In these cases, the most convenient solution of the problem consists in the separation of the different branches followed by appropriate investigation of the simplified network. The high correlation among parameters would otherwise invalidate any

reasonable conclusion when the overall approach is adopted. We have therefore determined the equilibrium constant between the complexes **1A** and **1C** and between the complexes **2A** and **2C** by spectrophotometric titration of the complex **1A** or **2A** with a CH_2Cl_2 solution of TEBA Cl (triethylbenzylammonium chloride).

Determination of Equilibrium Constants. The Equilibrium Constants.

$$K_E' = [\mathbf{1C}]/[\mathbf{1A}][\text{Cl}^-]$$

and

$$K_E'' = [\mathbf{2C}]/[\mathbf{2A}][\text{Cl}^-]$$

corresponding to the general equation $K_E = [\text{C}]/[\text{A}][\text{Cl}^-]^{22}$ were determined by means of nonlinear regression analysis of the total absorbance of the system upon addition of chloride, calculated on the basis of the following equations in the SCIENTIST environment:

$$[\text{C}] = K_E([\text{A}]_0 - [\text{C}])([\text{Cl}^-]_0 - [\text{C}]) \quad (1)$$

$$D_i = \varepsilon_C[\text{C}] + \varepsilon_A([\text{A}]_0 - [\text{C}]) \quad (2)$$

where $[\text{C}]$ represents the actual concentration of **1C** (or **2C**), $[\text{A}]_0$ the initial concentration of **1A** (or **2A**), and $[\text{Cl}^-]_0$ the concentration of TEBA Cl after each addition. D_i represents the optical density of the system at any chloride addition, while ε_A and ε_C are the molar extinction coefficients of the complexes involved in the titration. The ensuing K_E values determined as refined parameters together with ε_C were $K_E' = (6.7 \pm 0.9) \times 10^5$ and $K_E'' = (8.1 \pm 0.5) \times 10^3$, respectively, while the extinction coefficients ε_C were coincident with those experimentally determined from solutions of authentic **1C** or **2C** samples.

Determination of Rate Constants. Reactivity of 1A and 1C. As already stated, the network in Scheme 6 can be kinetically resolved by studying each step individually. Thus, the perchlorate salts of complex **1A** in the absence of chloride

(21) When the equilibrium between the complexes **2A** and **2C** in the presence of an equimolar amount of chloride is taken into consideration ($K_E'' = 8100$), the degree of advancement of the reaction is $\xi = 0.93$ at NMR concentration ($[\mathbf{2A}] = 2 \times 10^{-2} \text{ mol dm}^{-3}$) and $\xi = 0.35$ at UV–vis concentration ($[\mathbf{2A}] = 1 \times 10^{-4} \text{ mol dm}^{-3}$).

(22) The formulation of the equilibrium constant should require the knowledge of the concentrations of all the species in solution. Although such knowledge is not warranted in apolar solvents, we have somehow resorted to the classical and widely accepted semiquantitative expression.

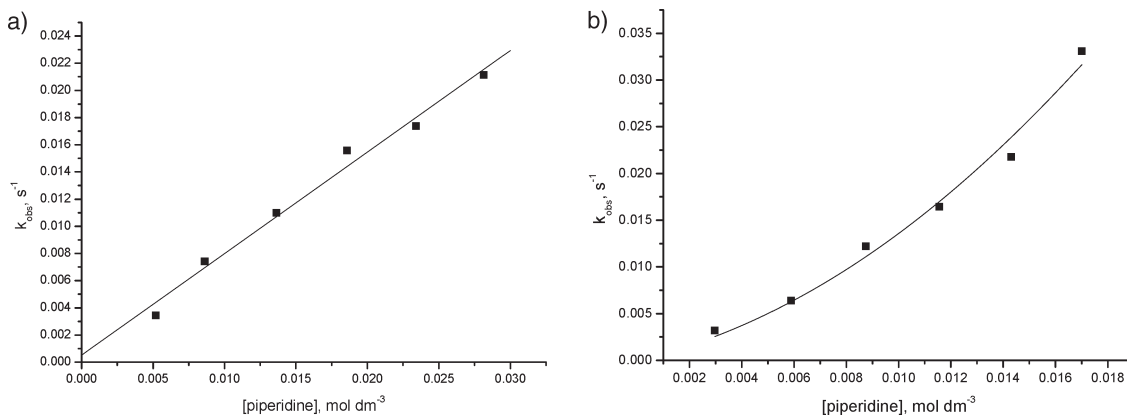


Figure 7. (a) Linear regression analysis for the reaction between complex **2C** and piperidine. (b) Parabolic regression analysis for the reaction between complex **2A** and piperidine.

and complex **1C** in the presence of TEBACl ($[\text{TEBACl}] = 10[\text{IC}]_0$) were reacted under spectrophotometric conditions (see Experimental Section) with solutions of piperidine under pseudo-first-order conditions ($[\text{piperidine}] \geq 10[\text{A}]_0$; $[\text{piperidine}] \geq 10[\text{C}]_0$). In the case of the determination of the reactivity of complex **1C** (k_2'), although the K_E' value ($K_E' = 6.7 \times 10^5$) under the described conditions ensures the complete displacement of the equilibrium position to the right with the consequent total transformation of **1A** into **1C** ($\xi = 1.00$), two kinetic measurements were repeated with increased TEBACl concentration ($[\text{TEBACl}] = 15 \times, 20 \times [\text{IC}]_0$) at the same piperidine concentration ($[\text{piperidine}] = 10 \times [\text{IC}]_0$). No significant differences among the k_{obs} were noticed, the ensuing values being comparable within 5%.

All the reactions went smoothly to completion and were fitted by the monoexponential equation

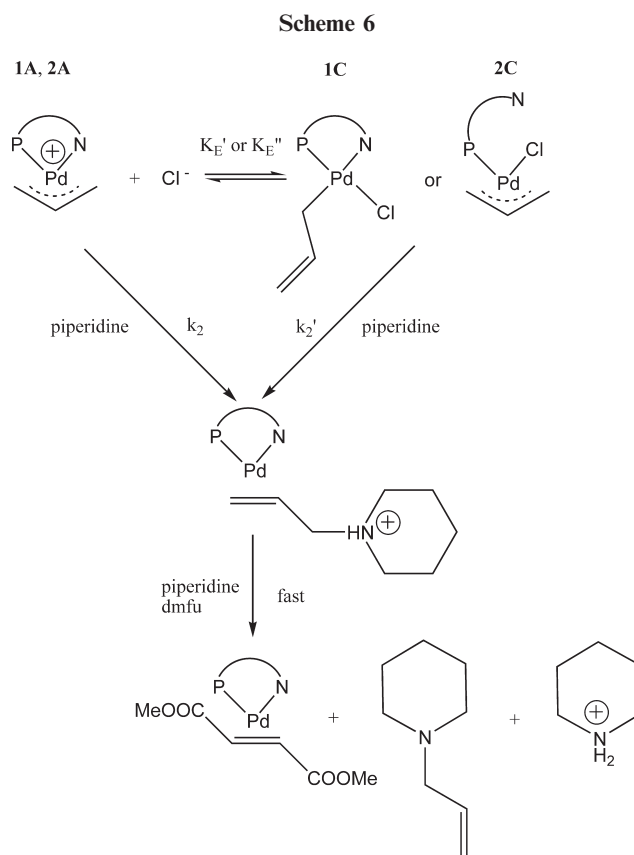
$$(D_t - D_\infty) = (D_0 - D_\infty) \exp(-k_{\text{obs}}t)$$

where D_0 , D_∞ , and D_t are the optical density at $t = 0$, at the end of reaction ($t = \infty$), and at time t . The ensuing k_{obs} values were fitted versus piperidine concentration, and the linear dependence shown in Figure 6a,b was observed for the complexes under study.

The linear regression in both cases is conveniently described by the equations $k_{\text{obs}} = k_2[\text{piperidine}]$ ($k_2 = (0.25 \pm 0.01) \text{ mol}^{-1} \text{ dm}^3 \text{ s}^{-1}$; **1A**) and $k_{\text{obs}} = k_2'[\text{piperidine}]$ ($k_2' = (1.44 \pm 0.07) \times 10^{-2} \text{ mol}^{-1} \text{ dm}^3 \text{ s}^{-1}$; **1C**). Complex **1C**, with the allyl fragment forced to η^1 -hapticity, displays a reaction rate about 20 times smaller than that of the “classical” η^3 -allyl complex **1A**.

Reactivity of 2A and 2C. The reaction of complex **2C** in the presence of TEBACl ($[\text{TEBACl}] = 10 \times [\text{2C}]$) with piperidine also obeys a simple monoexponential law. Again, the ensuing k_{obs} displays a linear dependence on piperidine concentration that is well described by the usual equation $k_{\text{obs}} = k_2[\text{piperidine}]$ ($k_2 = (0.74 \pm 0.04) \text{ mol}^{-1} \text{ dm}^3 \text{ s}^{-1}$; **2C**) (see Figure 7a). Apparently, complex **2C** reacts similarly to complex **1A** owing to the same η^3 -hapticity of the allyl moiety and almost irrespectively of the nature of the ancillary ligand, the differences between rate constants being insignificant.

Notably, complex **2A** reacts differently. In Figure 7b the parabolic dependence of k_{obs} on the piperidine concentration is clearly noticed. In keeping with the previously discussed behavior ascribable to the weakness of the bond between palladium and nitrogen of the DPPQ-Me molecule, we propose in this case the alternative mechanism depicted in Scheme 7.



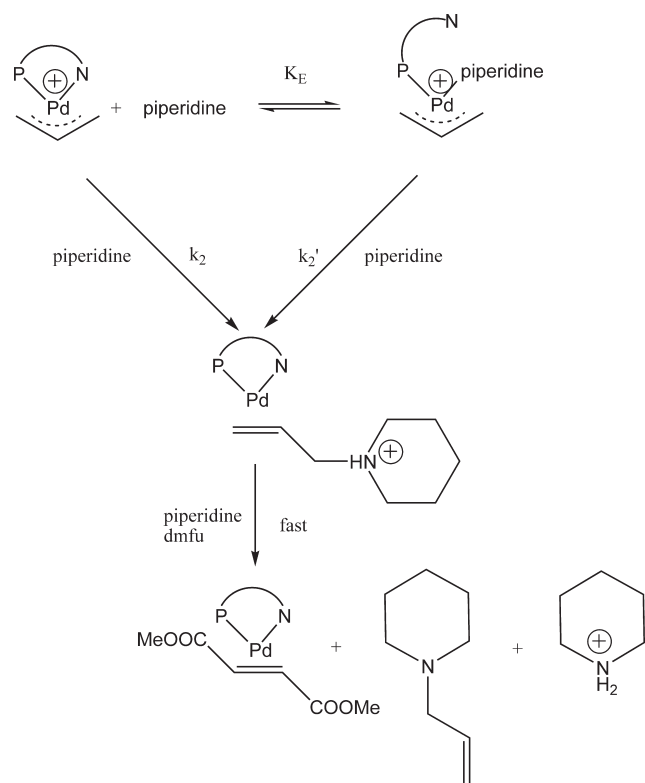
The overall reaction rate for the mechanism depicted in Scheme 7 is

$$k_{\text{obs}} = \frac{(k_2[\text{piperidine}] + k_2'K_E[\text{piperidine}]^2)}{(1 + K_E[\text{piperidine}])} \quad (1)$$

which reduces to the equation $k_{\text{obs}} = k_2[\text{piperidine}] + k_2'K_E[\text{piperidine}]^2$ when the term $K_E[\text{piperidine}]$ is negligible with respect to 1.²³ The ensuing values for k_2 and $k_2'K_E$ are 0.6 ± 0.2 and $70 \pm 15 \text{ mol}^{-1} \text{ dm}^3 \text{ s}^{-1}$, respectively. This finding is not unprecedented and was already observed in reactions between palladium iminophosphine allyl derivatives and secondary

(23) In the case in which one could be ignored ($1 \ll K_E$) with respect to the term $K_E[\text{piperidine}]$, eq 1 would become a straight line.

Scheme 7



aliphatic amines.^{8b} The small K_E value is confirmed by the impossibility of detecting any appreciable formation of the complex $[\text{Pd}(\eta^3\text{-C}_3\text{H}_5)(\kappa^1\text{-DPPQ-Me})(\text{piperidine})]$ by NMR technique when piperidine is added to the complex $[\text{Pd}(\eta^3\text{-C}_3\text{H}_5)(\text{DPPQ-Me})]\text{ClO}_4$. Moreover, similar values between the reaction constants of the complexes **2A** and **2C** (0.6 vs 0.74) suggest that substitution of a chloride ion in a neutral substrate by piperidine with the consequent formation of a cationic species hardly affects the reactivity of the derivatives, which probably depends on the allyl hapticity.

Conclusions

We have prepared some new allyl complexes of palladium with two phosphoquinoline ligands. Taking advantage of the nature of the two different ligands, we have synthesized six derivatives bearing the allyl fragment with its typical η^3 -hapticity and two with the allyl η^1 -coordinated.

We have found that formation of η^1 -allyl derivatives of palladium with potentially bidentate ligands is promoted by (i) the enhancement of the halide coordinative capability promoted by the use of an aprotic solvent (CH_2Cl_2 , CHCl_3); (ii) the presence of the strong *trans*-labilizing phosphorus atom weakening the Pd–C bond *trans* to it; and (iii) the weak tendency of the bidentate ligand to act as monodentate.

Point (i) arises from the observation that in MeOH the solvated chloride does not coordinate at palladium and acts only as a counterion. Point (ii) represents experimental evidence that confirms the literature findings.^{5d–h} As for point (iii), it was noticed that in the presence of chloride the DPPQ ligand, which has no tendency for monocoordination, forces the allyl group to η^1 -hapticity. On the contrary, the ligand DPPQ-Me, owing to the distortion induced by the methyl group in the complex frame, in the presence of

chloride tends to give monocoordination, and consequently derivatives bearing the allyl fragment are η^3 -coordinated.

A diffractometric study of the complexes **1A** and **1C** was also carried out. The resolved structure of **1C** represents one of the few examples of η^1 -coordinated allyl fragments in the literature.

The reactivity of the allyl derivatives toward allyl amination was also investigated and in some cases studied in detail by NMR and UV–vis techniques. It was shown that the η^1 -allyl derivatives react slowly with respect to their η^3 -counterparts. From NMR experiments it was also shown that the η^1 - $\text{C}_3\text{H}_3\text{Me}_2$ derivative, besides the reduced reactivity, displays a significant inversion in the regioselectivity dictated by the preferential attack of piperidine to the most substituted allyl termini ($\text{S}_{\text{N}}2'$), although the $\text{S}_{\text{N}}2$ path is also operative.

Experimental Section

Computational Details. Theoretical calculations were performed with the Gaussian 09¹³ package using the functional hybrid meta-GGA M06^{14a} and the Def2-TZVP basis set.^{14b} The geometry optimization was performed without any symmetry constraint, followed by analytical frequency calculation to confirm that a minimum or a transition state had been reached.

Nonlinear and linear analysis of the data related to equilibrium and kinetics measurements were performed by locally adapted routines written in ORIGIN 7.5 or SCIENTIST environments.

Crystal Structure Determination. The crystal data of compounds **1C** and **1A** were collected at room temperature using a Nonius Kappa CCD diffractometer with graphite-monochromated Mo K α radiation. The data sets were integrated with the Denzo-SMN package²⁴ and corrected for Lorentz, polarization, and absorption effects (SORTAV).²⁵ The structures were solved by direct methods using the SIR97²⁶ system of programs and refined using full-matrix least-squares with all non-hydrogen atoms anisotropically refined and hydrogens included on calculated positions, riding on their carrier atoms, except for the hydrogens of the allyl moiety in compound **1C**, which were refined isotropically. In compound **1A** the O2, O3, and O4 oxygens of ClO_4^- anion are disordered and refined over two positions with occupancies of 0.5 each.

All calculations were performed using SHELXL-97²⁷ and PARST²⁸ implemented in the WINGX²⁹ system of programs. The crystal data and selected bond distances and angles are reported as Table 1 SI and Table 2 SI, respectively, in the Supporting Information.

Kinetic Measurements (NMR). The kinetics of attack of piperidine on allyl palladium complexes were carried out by means of ^1H or ^{31}P NMR techniques under the following experimental conditions: $[\text{complex}] = 2 \times 10^{-2}$, $[\text{piperidine}] = 1 \times 10^{-1}$, and $[\text{dmfu}] = 2.4 \times 10^{-2} \text{ mol dm}^{-3}$.

The reactions were monitored by recording ^1H or ^{31}P NMR spectra as a function of time (time = 0 at piperidine addition).

Equilibrium Measurements. The equilibrium constants K_E were obtained by spectrophotometric titration of 50 mL of a solution of the complex $[\text{Pd}(\eta^3\text{-C}_3\text{H}_5)(\text{DPPQ})]$ ($[\mathbf{1A}] = 1 \times 10^{-4} \text{ mol dm}^{-3}$) or $[\text{Pd}(\eta^3\text{-C}_3\text{H}_5)(\text{DPPQ-Me})]$ ($[\mathbf{2A}] = 9.53 \times 10^{-5} \text{ mol dm}^{-3}$) with

(24) Otwinowski, Z.; Minor, W. In *Methods in Enzymology*; Carter, C. W.; Sweet, R. M. Eds.; Academic Press: London, 1997; Vol. 276, Part A, pp 307–326.

(25) Blessing, R. H. *Acta Crystallogr., Sect. A* **1995**, *51*, 33–38.

(26) Altomare, A.; Burla, M. C.; Camalli, M.; Cascarano, G. L.; Giacovazzo, C.; Guagliardi, A.; Moliterni, A. G.; Polidori, G.; Spagna, R. *J. Appl. Crystallogr.* **1999**, *32*, 115–119.

(27) Sheldrick, G. M. *SHELX-97*, Program for Crystal Structure Refinement; University of Gottingen: Germany, 1997.

(28) Nardelli, M. *J. Appl. Crystallogr.* **1995**, *28*, 659–659.

(29) Farrugia, L. J. *J. Appl. Crystallogr.* **1999**, *32*, 837–838.

microaliquots of a concentrated CH_2Cl_2 solution of TEBACl. The ensuing spectra were recorded in the 300–450 nm wavelength range.

Kinetic Measurements (UV–Vis). The kinetic measurements were performed by adding microaliquots of a concentrated CH_2Cl_2 solution of piperidine to 3 mL of the complex under study ($[\text{complex}] = 1 \times 10^{-4} \text{ mol dm}^{-3}$) in the presence of dmfu ($[\text{dmfu}] = 3 \times 10^{-4} \text{ mol dm}^{-3}$) and in the presence of TEBACl ($[\text{TEBACl}] = 1 \times 10^{-3}, 1.5 \times 10^{-3}, 2 \times 10^{-3} \text{ mol dm}^{-3}$; determination of k_2') or in the absence of TEBACl ($[\text{TEBACl}] = 0 \text{ mol dm}^{-3}$; determination of k_2). The reactions were monitored by recording the UV–vis spectra as a function of time at the wavelength of the largest absorbance change (327 nm).

Materials. All solvents were purified by standard procedures and distilled under argon immediately prior to use. 1D- and 2D-NMR spectra were recorded using a Bruker 300 Avance spectrometer. Chemical shifts (ppm) are given relative to TMS (^1H and ^{13}C NMR) and 85% H_3PO_4 (^{31}P NMR). Peaks are labeled as singlet (s), doublet (d), triplet (t), quartet (q), multiplet (m), and broad (br). The proton and carbon assignment was performed by ^1H -2D COSY, ^1H -2D NOESY, ^1H - ^{13}C HMQC, and HMBC experiments. UV–vis spectra were recorded on a Perkin-Elmer Lambda 40 spectrophotometer equipped with a Perkin-Elmer PTP 6 (Peltier temperature programmer) apparatus. IR spectra were recorded on a Perkin-Elmer Spectrum One spectrophotometer. DPPQ, $^{30}\text{DPPQ-Me}$, $^{31}\text{[Pd}(\mu\text{-Cl})(\eta^3\text{-C}_3\text{H}_5)_2\text{]}_2$, and $^{32}\text{[Pd}(\mu\text{-Cl})(\eta^3\text{-C}_3\text{H}_5)_2\text{]}_2$ were prepared following literature procedures. All other chemicals were commercial grade and were used without further purification.

Synthesis of the Complexes. $^{31}\text{[Pd}(\eta^3\text{-C}_3\text{H}_5)(\text{DPPQ})\text{]}^+\text{ClO}_4^-$ (**1A**). To 0.0518 g (0.1416 mmol) of $^{31}\text{[Pd}(\mu\text{-Cl})(\eta^3\text{-C}_3\text{H}_5)_2\text{]}$ dissolved in 5.5 mL of CH_2Cl_2 were added 0.090 g (0.2872 mmol) of DPPQ in 3 mL of CH_2Cl_2 and 0.0785 g (0.5589 mmol) of NaClO_4 in 3 mL of MeOH. The resulting solution was stirred for 30 min and taken to dryness under vacuum. The residue was dissolved in CH_2Cl_2 and the undissolved NaCl filtered off. The resulting clear solution was treated with activated charcoal, filtered on a Celite filter, and concentrated to a small volume. Addition of diethyl ether induced the precipitation of 0.1468 g of yellow microcrystals, which were filtered into a Gooch and washed with diethyl ether and *n*-pentane (yield = 93%). ^1H NMR (300 MHz, CD_2Cl_2 , $T = 213 \text{ K}$, ppm): δ 2.97 (d, 1H, $J = 12.6 \text{ Hz}$, allyl $\text{H}_{\text{anti trans-N}}$), 4.08 (d, 1H, $J = 6.0 \text{ Hz}$, allyl $\text{H}_{\text{syn trans-N}}$), 4.29 (dd, 1H, $J = 12.0 \text{ Hz}$, $J_{\text{PH}} = 9.3 \text{ Hz}$, allyl $\text{H}_{\text{anti trans-P}}$), 5.04 (dd, 1H, $J = 7.0 \text{ Hz}$, $J_{\text{PH}} = 7.0 \text{ Hz}$, allyl $\text{H}_{\text{syn trans-P}}$), 6.03 (m, 1H, allyl $\text{H}_{\text{central}}$), 7.49–7.57 (m, 10 H, PPh_2), 7.83–7.90 (m, 2H, H^3 , H^6), 8.11 (m, 1H, H^7), 8.28 (d, 1H, $J = 8.10 \text{ Hz}$, H^5), 8.71 (dd, 1H, $J = 9.0 \text{ Hz}$, $J_{\text{PH}} = 1.2 \text{ Hz}$, H^4), 9.51 (d, 1H, $J = 4.8 \text{ Hz}$, H^2). $^{13}\text{C}\{^1\text{H}\}$ NMR (CD_2Cl_2 , $T = 298 \text{ K}$, ppm): δ 51.9 (CH_2 , allyl *trans-N*), 83.2 (d, CH_2 , $J_{\text{CP}} = 29.2 \text{ Hz}$, allyl *trans-P*), 123.0 (d, CH, $J_{\text{CP}} = 6.5 \text{ Hz}$, allyl $\text{C}_{\text{central}}$), 123.9 (CH, C^3), 128.6 (d, CH, $J_{\text{CP}} = 6.6 \text{ Hz}$, C^6), 131.9 (d, C, $J_{\text{CP}} = 42.8 \text{ Hz}$, C^8), 133.1 (CH, C^5), 138.9 (CH, C^7), 140.8 (CH, C^4), 151.0 (C, C^{10}), 151.3 (C, C^9), 160.0 (C, C^2). $^{31}\text{P}\{^1\text{H}\}$ NMR (300 MHz, CD_2Cl_2 , $T = 298 \text{ K}$, ppm): δ 32.45. IR (KBr pellet): $\nu_{\text{CN}} 1606, 1582, 1572 \text{ cm}^{-1}$; $\nu_{\text{ClO}} 1088 \text{ cm}^{-1}$, $\delta_{\text{ClO}} = 624 \text{ cm}^{-1}$.

The following complexes were synthesized following a similar procedure using the appropriate starting complexes and ancillary ligands.

$^{31}\text{[Pd}(\eta^3\text{-C}_3\text{H}_5)_2(\text{DPPQ})\text{]}^+\text{ClO}_4^-$ (**1B**): yellow ochre microcrystals (yield = 89%). Isomer **1B(a)**. ^1H NMR (300 MHz, CD_2Cl_2 , $T = 253 \text{ K}$, ppm): δ 1.67 (d, 3H, $J_{\text{PH}} = 6.0 \text{ Hz}$, allyl $-\text{CH}_{3\text{anti}}$), 2.19 (d, 3H, $J_{\text{PH}} = 9.9 \text{ Hz}$, allyl $-\text{CH}_{3\text{syn}}$), 3.08 (s, 1H, allyl $\text{H}_{\text{anti trans-N}}$), 3.77 (s, 1H, allyl $\text{H}_{\text{syn trans-N}}$), 5.51 (m, 1H, $\text{H}_{\text{central}}$), 9.08 (d, 1H, $J_{\text{HH}} = 4.8 \text{ Hz}$, H^2). $^{31}\text{P}\{^1\text{H}\}$ NMR

(300 MHz, CD_2Cl_2 , $T = 298 \text{ K}$, ppm): δ 33.97. Isomer **1B(b)**. ^1H NMR (300 MHz, CD_2Cl_2 , $T = 253 \text{ K}$, ppm): δ 1.14 (d, 3H, $J_{\text{PH}} = 6.3 \text{ Hz}$, allyl $-\text{CH}_{3\text{anti}}$), 1.69 (d, 3H, $J_{\text{PH}} = 9.0$, allyl $-\text{CH}_{3\text{syn}}$), 4.22 (dd, 1H, $J = 14.4 \text{ Hz}$, $J_{\text{PH}} = 10.2 \text{ Hz}$, allyl $\text{H}_{\text{anti trans-P}}$), 4.74 (dd, 1H, $J = 7.5 \text{ Hz}$, $J_{\text{PH}} = 7.5 \text{ Hz}$, allyl $\text{H}_{\text{syn trans-P}}$), 5.87 (m, 1H, $\text{H}_{\text{central}}$), 9.53 (d, 1H, $J = 4.8 \text{ Hz}$, H^2). $^{31}\text{P}\{^1\text{H}\}$ NMR (300 MHz, CD_2Cl_2 , $T = 298 \text{ K}$, ppm): δ 27.56. IR (KBr pellet): $\nu_{\text{CN}} 1607, 1583, 1573 \text{ cm}^{-1}$; $\nu_{\text{ClO}} 1093 \text{ cm}^{-1}$, $\delta_{\text{ClO}} = 622 \text{ cm}^{-1}$.

$^{31}\text{[Pd}(\eta^3\text{-C}_3\text{H}_5)(\text{DPPQ-Me})\text{]}^+\text{ClO}_4^-$ (**2A**): yellow ochre microcrystals (yield = 92%). ^1H NMR (300 MHz, CD_2Cl_2 , $T = 213 \text{ K}$, ppm): δ 2.95 (d, 1H, $J = 12.3 \text{ Hz}$, allyl $\text{H}_{\text{anti trans-N}}$), 3.04 (s, 3H, CH_3), 3.93 (d, 1H, $J = 7.2 \text{ Hz}$, allyl $\text{H}_{\text{syn trans-N}}$), 4.09 (dd, 1H, $J = 15.0 \text{ Hz}$, $J_{\text{PH}} = 9.6 \text{ Hz}$, allyl $\text{H}_{\text{anti trans-P}}$), 5.33 (dd, 1H, $J = 7.2 \text{ Hz}$, $J_{\text{PH}} = 7.0 \text{ Hz}$, allyl $\text{H}_{\text{syn trans-P}}$), 5.85 (m, 1H, allyl $\text{H}_{\text{central}}$), 7.43–7.62 (m, 10H, 10 PPh_2), 7.79 (m, 2H, H^7_{qui} , H^3_{qui}), 7.87 (m, 1H, H^6_{qui}), 8.22 (d, 1H, $J_{\text{HH}} = 7.8 \text{ Hz}$, H^5), 8.54 (dd, 1H, $J_{\text{HH}} = 8.4 \text{ Hz}$, $J_{\text{HH}} = 1.8 \text{ Hz}$, H^4). $^{13}\text{C}\{^1\text{H}\}$ NMR (CD_2Cl_2 , $T = 298 \text{ K}$, ppm): δ 33.0 (CH_3), 52.8 (CH_2 , allyl *trans-N*), 84.2 (d, CH_2 , $J_{\text{CP}} = 30.8 \text{ Hz}$, allyl *trans-P*), 119.9 (d, CH, $J_{\text{CP}} = 6.5 \text{ Hz}$, allyl $\text{C}_{\text{central}}$), 124.5 (CH, C^3), 127.6 (d, CH, $J_{\text{CP}} = 6.8 \text{ Hz}$, C^6), 130.5 (d, C, $J_{\text{CP}} = 42.0 \text{ Hz}$, C^8), 132 (CH, C^5), 138.0 (CH, C^7), 140.6 (CH, C^4), 151.7 (C, C^{10}), 151.9 (C, C^9), 164.9 (C, C^2). $^{31}\text{P}\{^1\text{H}\}$ NMR (300 MHz, CD_2Cl_2 , $T = 298 \text{ K}$, ppm): δ 34.05. IR (KBr pellet): $\nu_{\text{CN}} 1605 \text{ cm}^{-1}$; $\nu_{\text{ClO}} 1088 \text{ cm}^{-1}$; $\delta_{\text{ClO}} = 624 \text{ cm}^{-1}$.

$^{31}\text{[Pd}(\eta^3\text{-C}_3\text{H}_5)_2(\text{DPPQ-Me})\text{]}^+\text{ClO}_4^-$ (**2B**): yellow ochre microcrystals (yield = 89%). Isomer **2B(a)**. ^1H NMR (300 MHz, CD_2Cl_2 , $T = 298 \text{ K}$, ppm): δ 1.68 (d, 3H, $J_{\text{PH}} = 7.2 \text{ Hz}$, allyl $-\text{CH}_{3\text{anti}}$), 2.19 (d, 3H, $J_{\text{PH}} = 12.0 \text{ Hz}$, allyl $-\text{CH}_{3\text{syn}}$), 2.8 bs (2H, H_{syn} , $\text{H}_{\text{anti trans N}}$), 3.09 (s, 3H, $\text{CH}_{3\text{qui}}$), 5.49 (t, 1H, $J = 9.9 \text{ Hz}$, allyl $\text{H}_{\text{central}}$), 7.92 (m, 1H, H^7), 8.22 (d, 1H, $J = 7.91 \text{ Hz}$, H^5), 8.52 (d, 1H, $J = 8.6 \text{ Hz}$, H^4). $^{31}\text{P}\{^1\text{H}\}$ NMR (300 MHz, CD_2Cl_2 , $T = 298 \text{ K}$, ppm): δ 36.32. Isomer **2B(b)**. ^1H NMR (300 MHz, CD_2Cl_2 , $T = 298 \text{ K}$, ppm): δ 1.13 (d, 3H, $J_{\text{PH}} = 6.9 \text{ Hz}$, allyl $-\text{CH}_{3\text{anti}}$), 1.46 (d, 3H, $J_{\text{PH}} = 10.2 \text{ Hz}$, allyl $-\text{CH}_{3\text{syn}}$), 3.09 (s, 3H, $\text{CH}_{3\text{qui}}$), 4.02 (dd, 1H, $J = 14.5 \text{ Hz}$, $J_{\text{PH}} = 10.5 \text{ Hz}$, allyl $\text{H}_{\text{anti trans-P}}$), 4.97 (dd, 1H, $J = 8.1 \text{ Hz}$, $J_{\text{PH}} = 8.1 \text{ Hz}$, allyl $\text{H}_{\text{syn trans-P}}$), 5.66 (m, 1H, allyl $\text{H}_{\text{central}}$), 8.01 (m, 1H, H^7), 8.20 (d, 1H, $J = 8.1 \text{ Hz}$, H^5), 8.49 (d, 1H, $J = 8.6 \text{ Hz}$, H^4). $^{31}\text{P}\{^1\text{H}\}$ NMR (300 MHz, CD_2Cl_2 , $T = 298 \text{ K}$, ppm): δ 31.02. IR (KBr pellet): $\nu_{\text{CN}} 1605 \text{ cm}^{-1}$; $\nu_{\text{ClO}} 1095 \text{ cm}^{-1}$; $\delta_{\text{ClO}} = 623 \text{ cm}^{-1}$.

$^{31}\text{[Pd}(\eta^1\text{-C}_3\text{H}_5)(\text{DPPQCl})\text{]}^+\text{ClO}_4^-$ (**1C**). To 0.0495 g (0.1353 mmol) of $^{31}\text{[Pd}(\mu\text{-Cl})(\eta^3\text{-C}_3\text{H}_5)_2\text{]}$ dissolved in 20 mL of anhydrous CH_2Cl_2 was added 0.0864 g (0.2757 mmol) of DPPQ under inert atmosphere and in an ice bath. The solution was stirred for 15 min and evaporated under vacuum to small volume. Addition of diethyl ether induced the precipitation of 0.1222 g of the title complex as dark yellow microcrystals, which were filtered into a Gooch and dried under vacuum (yield = 91%). ^1H NMR (300 MHz, CD_2Cl_2 , $T = 223 \text{ K}$, ppm): δ 2.61 (dd, 2H, $J_{\text{HH}} = 12.0 \text{ Hz}$, $J_{\text{PH}} = 3.9 \text{ Hz}$, Pd- CH_2), 4.04 (d, 1H, $J = 16.8 \text{ Hz}$, $=\text{CH}_{2\text{trans}}$), 4.32 (d, 1H, $J = 9.9$, $=\text{CH}_{2\text{cis}}$), 6.09 (m, 1H, $=\text{CH}$), 7.46–7.49 (m, 6H, 6 PPh_2), 7.67–7.78 (m, 6 H, 4 PPh_2 , H^6 , H^3), 8.11–8.14 (m, 2H, H^7 , H^5), 8.47 (d, 1H, $J = 8.4 \text{ Hz}$, H^4), 9.89 (d, 1H, $J = 6.6 \text{ Hz}$, H^2). $^{13}\text{C}\{^1\text{H}\}$ NMR (CD_2Cl_2 , $T = 298 \text{ K}$, ppm): δ 19.7 (CH_2 , Pd- CH_2), 107.3 (CH_2 , $=\text{CH}_2$), 123.1 (CH, C^3), 127.8 (d, CH, $J_{\text{CP}} = 6.9 \text{ Hz}$, C^6), 132.1 (CH, C^5), 133.9 (C, $J_{\text{CP}} = 44.9 \text{ Hz}$, C^8), 136.7 (CH, C^7), 138.7 (CH, C^4), 141.6 (CH, $=\text{CH}$), 149.9 (C, C^{10}), 150.2 (C, C^9), 153.6 (CH, C^2). $^{31}\text{P}\{^1\text{H}\}$ NMR (300 MHz, CD_2Cl_2 , $T = 298 \text{ K}$, ppm): δ 38.54. IR (KBr pellet): $\nu_{\text{CN}} 1603, 1589, 1570 \text{ cm}^{-1}$.

The following complexes were synthesized following a similar procedure using the appropriate starting complexes and ancillary ligands.

$^{31}\text{[Pd}(\eta^1\text{-C}_3\text{H}_5)_2(\text{DPPQCl})\text{]}^+\text{ClO}_4^-$ (**1D**): dark yellow microcrystals (yield = 87%). ^1H NMR (300 MHz, CDCl_3 , $T = 298 \text{ K}$, ppm): δ 1.19 (s, 3H, $=\text{CCH}_{3\text{trans}}$), 1.40 (d, 3H, $J = 2.4 \text{ Hz}$, $=\text{CCH}_{3\text{cis}}$), 2.89 (d, 2H, $J = 6.9 \text{ Hz}$, Pd- CH_2), 5.47 (t, 1H, $J = 6.9 \text{ Hz}$, $\text{H}_{\text{central}}$), 7.41–7.54 (m, 6H, 6 PPh_2), 7.61–7.68 (m, 2H, H^3 , H^6), 7.70–7.79 (m, 4H, 4 PPh_2), 7.94 (m, 1H, H^7), 8.02 (d, 1H, $J = 8.1 \text{ Hz}$, H^5),

(30) Wehman, P.; van Donge, H. M. A.; Hagos, A.; Kamer, P. C. *J. Organomet. Chem.* **1997**, *535*, 183–193.

(31) Canovese, L.; Visentin, F.; Chessa, G.; Uguagliati, P.; Santo, C.; Dolmella, A. *Organometallics* **2005**, *24*, 3297–3308.

(32) Hartley, F. R.; Jones, S. R. *J. Organomet. Chem.* **1974**, *66*, 465–473.

(33) Auburn, P. R.; Mackenzie, P. B.; Bosnich, B. *J. Am. Chem. Soc.* **1985**, *107*, 2033–2046.

8.34 (d, 1H, $J = 8.1$ Hz, H⁴), 10.03 (d, 1H, $J = 4.8$ Hz, H²). ¹³C{¹H} NMR (CD₂Cl₂, $T = 298$ K, ppm): δ 15.6 (CH₂, =CH₂), 18.4 (CH₃, =C-CH₃ *trans*), 26.6 (CH₃, =C-CH₃ *cis*), 122.9 (CH, C³), 127.4 (d, CH, $J_{CP} = 6.7$ Hz, C⁶), 129.0 (s, CH, =CH), 131.5 (CH, C⁵), 135.3 (d, CH, $J_{CP} = 43.8$ Hz, C⁸), 136.0 (CH, C⁷), 138.0 (CH, C⁴), 149.6 (C, C¹⁰), 149.9 (C, C⁹), 153.7 (CH, C²). ³¹P{¹H} NMR (300 MHz, CD₂Cl₂, $T = 298$ K, ppm): δ 35.45. IR (KBr pellet): ν_{CN} 1634, 1592, 1570 cm⁻¹.

[Pd(η^3 -C₃H₅)(κ^1 -DPPQ-Me)Cl] (**2C**): yellow ochre microcrystals (yield = 88%). ¹H NMR (300 MHz, CD₂Cl₂, $T = 298$ K, ppm): δ 2.72 (s, 3H, CH₃), 3.65 (dd, 4H, $J = 12.0$ Hz, $J_{PH} = 3.9$ Hz, allyl H_{anti} *trans*-N, allyl H_{syn} *trans*-N, allyl H_{anti} *trans*-P, allyl H_{syn} *trans*-P), 5.67 (m, 1H, allyl C_{central}), 7.68–7.39 (m, 13H, 10 PPh₂, H⁷, H³, H⁶), 8.02 (d, 1H, $J_{HH} = 7.8$ Hz, H⁵), 8.25 (dd, 1H, $J = 9.0$ Hz, $J = 1.5$ Hz, H⁴). ¹³C{¹H} NMR (CD₂Cl₂, $T = 298$ K, ppm): δ 28.2 (CH₃, -CH₃_{qui}), 68.6 bs (2 CH₂, allyl *trans*-P, allyl *trans*-N), 118.9 (d, CH, $J_{CP} = 5.8$ Hz, allyl C_{central}), 123.5 (CH, C³), 128.6 (d, CH, $J_{CP} = 4.3$ Hz, C⁶), 131.3 (C, C⁵), 135.5 (CH, C⁷), 136.2 (CH, $J_{CP} = 2.8$ Hz, C⁸), 137.7 (CH, C⁴), 149.4 (C, C¹⁰), 152.6 (C, C⁹), 161.2 (C, C²). ³¹P{¹H} NMR (300 MHz, CD₂Cl₂, $T = 298$ K, ppm): δ 22.69. IR (KBr pellet): ν_{CN} 1602 cm⁻¹.

[Pd(η^3 -C₃H₃Me₂)(κ^1 -DPPQ-Me)Cl] (**2D**): light yellow microcrystals (yield = 78%). ¹H NMR (300 MHz, CD₂Cl₂, $T = 298$ K, ppm): δ 1.37 (d, 3H, $J_{PH} = 5.7$ Hz, allyl CH₃_{anti} *trans*-P), 1.80 (d, 3H, $J_{PH} = 8.7$ Hz, allyl CH₃_{syn} *trans*-P), 2.60 (s, 3H,

CH₃), 2.75 (d, 2H, $J = 9.9$ Hz, allyl H *trans*-Cl, allyl H *trans*-Cl), 5.19 (t, 1H, $J = 9.6$ Hz, $J = 9.9$ Hz, H_{central}), 7.23–7.30 (m, 1H, H⁷), 7.34–7.49 (m, 8H, H⁶, H³, 6 PPh₂), 7.64–7.73 (m, 4H, 4 PPh₂), 7.95 (d, 1H, $J = 8.1$ Hz, H⁵), 8.16 (d, 1H, $J = 9.3$ Hz, H⁴). ¹³C{¹H} NMR (CD₂Cl₂, $T = 298$ K, ppm): δ 20.3 (CH₃, -CH₃_{sym}), 25.1 (CH₃, -CH₃_{qui}), 26.0 (CH₃, -CH₃_{anti}), 48.9 (CH₂, allyl -CH₂), 111.4 (CH, C_{central}), 114.3 (C, -C(CH₃)₂), 122.6 (CH, C³), 125.2 (d, CH, $J_{CP} = 8.3$ Hz, C⁶), 130.3 (CH, C⁵), 133.3 (d, C, $J_{CP} = 44.7$ Hz, C⁸), 133.9 (s, CH, C⁷), 136.0 (CH, C⁴), 147.7 (C, C¹⁰), 147.8 (C, C⁹), 158.9 (CH, C²). ³¹P{¹H} NMR (300 MHz, CD₂Cl₂, $T = 298$ K, ppm): δ 23.34. IR (KBr pellet): ν_{CN} 1600 cm⁻¹.

Supporting Information Available: Crystallographic data (excluding structure factors) have been deposited at the Cambridge Crystallographic Data Centre and allocated the deposition numbers CCDC 771053–771054. These data can be obtained free of charge via www.ccdc.cam.ac.uk/conts/retrieving.html or on application to CCDC, 12 Union Road, Cambridge CB2 1EZ, UK [fax: (+44)1223-336033, e-mail: deposit@ccdc.cam.ac.uk]. Tables of crystallographic data (Table 1SI) and of the selected bond distances and angles (Table 2SI), NMR and IR spectra, and the nonlinear regression equilibrium fits are also reported. This material is available free of charge via the Internet at <http://pubs.acs.org>.